INTERNATIONAL JOURNAL OF FLUID POWER, 2017
VOL. 18, NO. 1, 17–28
http://dx.doi.org/10.1080/14399776.2016.1210423

A novel hydromechanical hybrid motion system for construction machines

Karl Pettersson[a], Kim Heybroek[c], Per Mattsson[a] and Petter Krus[b]

[a]Driveline Systems, Volvo Construction Equipment, Eskilstuna, Sweden; [b]Department of Management and Engineering, Linköping University, Linköping, Sweden; [c]Emerging Technologies, Volvo Construction Equipment, Eskilstuna, Sweden

ABSTRACT

This paper deals with a novel type of hybrid motion system for construction machines based on a common pressure rail shared between a hydromechanical power-split transmission and secondary controlled work hydraulics. A construction machine with driveline and work functions is a complex coupled motion system and the design of an effective hybrid system needs to take both subsystems into account. Studies on energy efficient hybrid systems for construction machines have hitherto principally focused on one subsystem at a time – work hydraulics or driveline. The paper demonstrates a use case with a specific transmission concept proposal for a medium-sized wheel loader. The system is modelled and simulated using an optimal energy management strategy based on dynamic programming. The results show the benefits of a throttle-free bidirectional link between the machine's subsystems and the energy storage, while taking advantage of the complex power flows of the power-split transmission.

ARTICLE HISTORY
Received 24 March 2016
Accepted 28 June 2016

KEYWORDS
Hydraulic hybrid; power-split; secondary control; wheel loader

Introduction

In an effort to reduce fuel consumption and increase the productivity of construction machines new innovative motion systems and hybridisation are continuously being investigated. In contrast to road vehicles, mobile working machines have several power consumers, i.e. machine functions, which must be considered in the system design. The design of hybrid motion systems for working machines is, in this sense, more challenging than for road vehicles with only one primary power consumer.

The wheel loader motion system consists of two parallel connected subsystems – driveline and work functions. The work functions and driveline commonly operate simultaneously and in all four quadrants of the force/speed diagram. There is also a tight coupling between the subsystems, since they are both mechanically connected to the engine shaft and thus interact during simultaneous operation. There is also an external coupling between the subsystems coming from the bucket interaction on the load. Consequently, if only one subsystem is targeted in the design of a new system concept the other might be negatively affected. A motion system capable of transferring power between the subsystems would, however, greatly improve the energy efficiency and reduce the requirements on storing recuperated energy. In (Filla 2009) some of the main subsystem interactions and operability aspects are explained for typical wheel loader operating cycles. Different hybrid topologies are also discussed and classified in a matrix for driveline and work functions based on the series, parallel and complex hybrid architectures. This paper proposes a new hybrid motion system based on secondary controlled hydraulic actuation and power-split technology.

Secondary controlled hydraulics

Secondary Controlled Systems (SCSs) are sometimes suggested as promising solution for throttle-free motion control. Secondary control has long been a research topic, but the technology has demonstrated promising results also in more recent publications, e.g. in Achten (2008), Pettersson and Tikkanen (2009) and Heybroek *et al.* (2012). In an SCS, the control is said to be moved closer to the load side. Instead of modulating the mechanical to hydraulic transformation on the supply side of the system, modulation takes place at the load side. The secondary controlled circuit often incorporates a hydraulic accumulator, resulting in the notion of a 'pressure coupling' between the supply and load side rather than a 'flow coupling'. The pressure coupling takes place in a common pressure rail (CPR) to which flow is provided by the supply side. At the load side, flow is either consumed or returned (recuperation). By nature, SCSs are ideally suited for rotary loads, using displacement control of pump/motors. However, in applying this technology to construction machines, secondary

CONTACT Karl Pettersson karl.pettersson.2@volvo.com
This article was originally published with errors. This version has been corrected. Please see Erratum (http://dx.doi.org/10.1080/14399776.2016.1218183)

controlled linear-mechanic actuators are required. One possible solution is the multi-chamber cylinder capable of varying the effective cylinder area in a stepwise manner. Examples of studies where this solution is considered for use in construction machinery can be found in Sipola *et al.* (2008) and Heybroek and Norlin (2015).

Power-split transmissions

Hydromechanical power-split transmissions are a powerful technology for heavy applications to achieve continuously variable transformation of rotational power with high efficiency. A power-split transmission combines a hydraulic variator with a mechanical power branch with the use of planetary gears. Part of the power is thus transferred over the mechanical branch, which in general has higher efficiency than a hydraulic power transfer. By using clutches the variator can be reused in different gear configurations to achieve higher power capacity and wider torque/speed range. Multiple mode power-split transmissions have for some time been state-of-the-art for agricultural tractors (Renius and Resch 2005). The technology has more recently been taken to material handling equipment and construction machinery (Stein *et al*. 2013). The main target for equipment manufacturers is to replace torque converter based transmissions and thereby reduce power losses generated by slip in the torque converter. A continuously variable transmission also decouples the engine and wheel speed to enable more efficient engine operating points.

Hydraulic hybrid power-split transmissions, often referred to as 'complex hybrids', have attracted increasing interest as they are seen as a viable alternative to series and parallel hybrids. Complex hybrids offer both highly efficient power transfer and engine-load decoupling at a competitive cost level (Kumar and Ivantysynova 2011).

Hybrid concept

Previous studies on series hydraulic hybrids for construction machinery, e.g. Heybroek *et al.* (2012), Inderelst *et al.* (2011) and Wei *et al.* (2013), have demonstrated that CPR-based motion systems with secondary controlled functions have great potential in terms of energy savings. Such systems allow for complete engine/load decoupling and advantageous operating points for the engine due to the high flexibility of the power management. Energy recuperation is possible for all machine functions. Additionally, the CPR functionality enables easy power transfer between the functions with minimal power transformation between physical domains, since all actuators are hydraulically driven. This is particularly useful for machines with parallel actuated functions with four quadrant load spectra, such as wheel loaders and excavators.

A hydraulic hybrid motion system is here proposed for a medium-sized wheel loader application. It consists of a CPR and secondary controlled work functions combined with a secondary controlled power-split driveline. This solution takes full advantage of the power-split technology while achieving the series hybrid motion system's functionality, demonstrated in the aforementioned references. The secondary controlled work functions can be realised with different solutions, one being a transformer-based system as shown in (Heybroek, et al., 2012). Figure 1 shows the proposed concept studied in this paper where the work functions are controlled by multi-chamber cylinders.

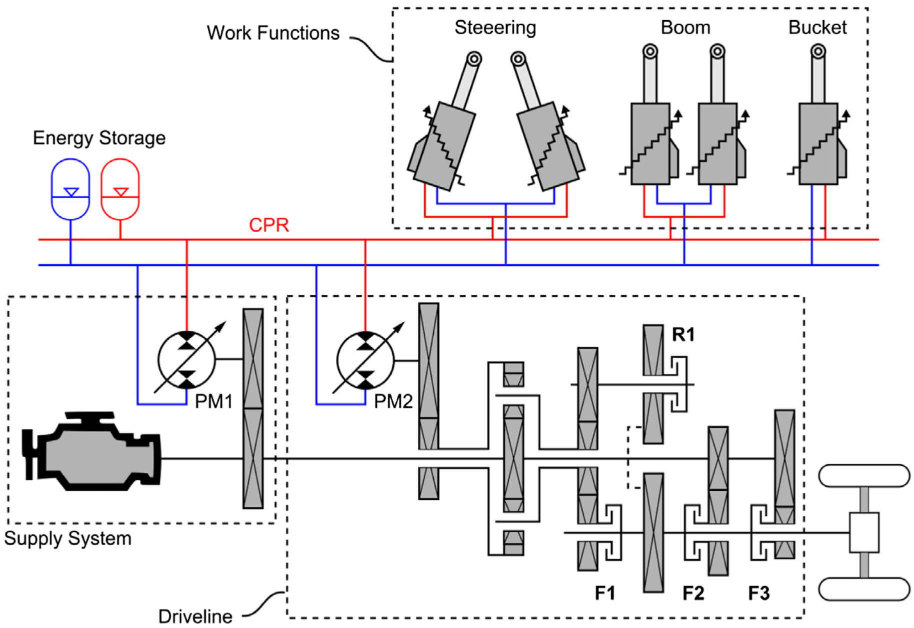

Figure 1. Proposed hybrid motion system concept for a medium sized wheel loader.

The driveline here consists of a partially continuously variable transmission with two power-split modes (*R*1 and *F*1) and two 'direct drives' (*F*2 and *F*3) used for transportation. The supply system, consisting of the engine and the primary pump/motor *PM*1, supplies the driveline and work functions with mechanical and hydraulic power by controlling the CPR pressure. *PM*1 is also a part of the hydraulic variator in the power-split transmission together with the secondary pump/motor, *PM*2. Two pressure levels are used in the CPR, each connected to a hydraulic accumulator, where the high pressure accumulator is the main device for storing energy. Besides increased capabilities to transfer energy between the machine functions, this concept requires one pump/motor less than hydraulic hybrid wheel loaders with separated subsystems, such as the system studied in (Wang, et al., 2016).

Work functions

The work functions in the hybrid concept are all actuated by Variable Displacement Linear Actuators (VDLAs). This technology was first introduced by Linjama *et al.* (2009) and is based on a cylinder with four chambers instead of two. The output force depends on which pressures are applied to which cylinder area. When all four cylinder areas differ in size and the CPR contains two pressure levels, the steady-state force combinations add up to $2^4 = 16$ steps. The CPR pressure differential acting on the cylinder translates to a stepwise variable cylinder output force. Directly mounted on the four-chamber cylinder is a valve manifold containing the necessary connections between its chambers and the CPR, as illustrated in Figure 2.

The possibility to throttle between the steady-state force steps allows for a more fine-grained force control. The drawback of this control approach is naturally the additional throttle losses that arise between the steps. Control loss is nonetheless expected to be relatively small, especially since accurate speed control is normally needed only at low speeds where the flows are low.

Driveline

The driveline is designed to take full advantage of the power-split functionality at low machine speeds. In this operating range, there is a complete decoupling of the engine and the vehicle speed while maintaining a high efficiency of the transmission. At higher speeds, the direct drives are activated similar to the lock-up function

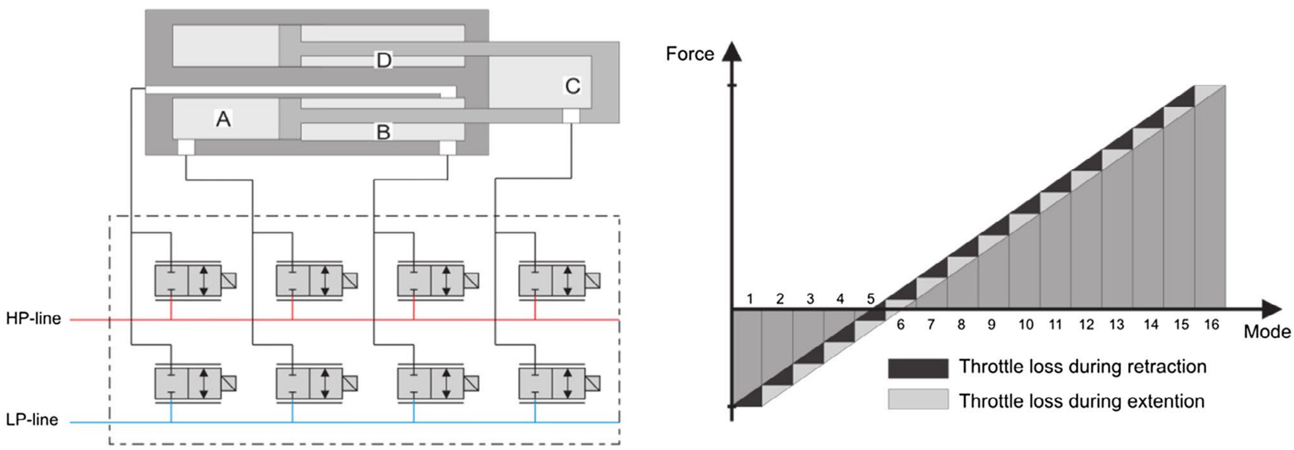

Figure 2. Steady-state force outputs for the four-chamber cylinder connected to the CPR through a valve manifold (Heybroek & Norlin, 2015).

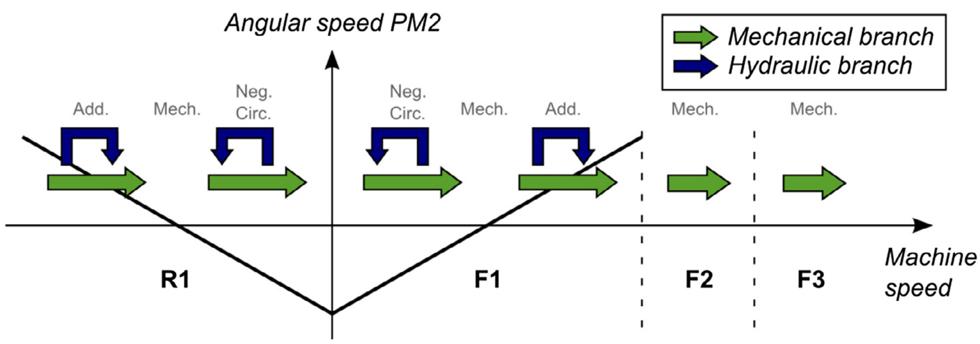

Figure 3. Principle of the driveline operation.

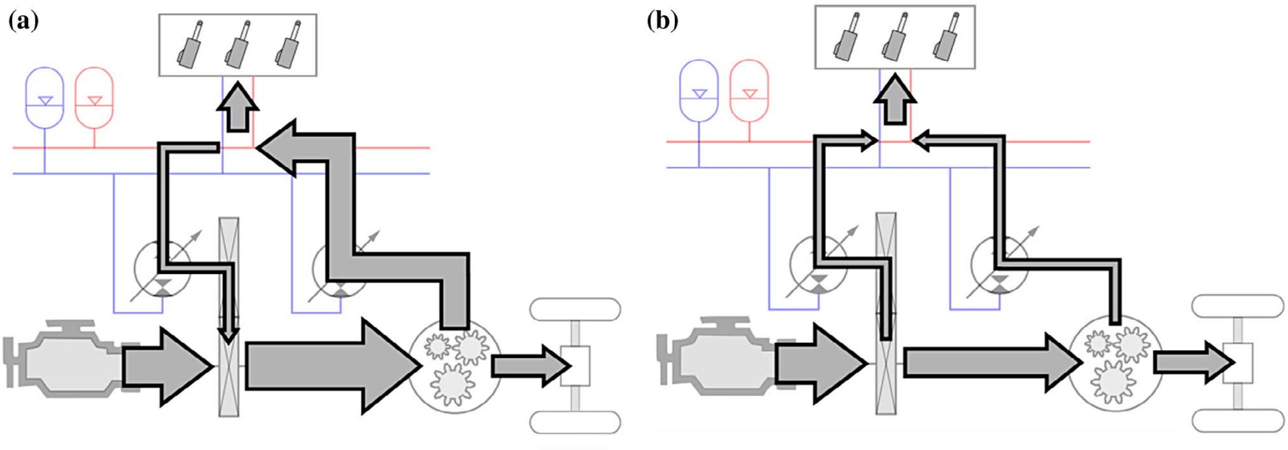

Figure 4. Negative circulating power when work functions and driveline output positive power and pressure is kept constant. (a) The circulating power is higher than the required power output of the work functions and the surplus power is fed back to the driveline. (b) The circulating power is lower than the required power output of the work functions and PM1 supplies the remaining power.

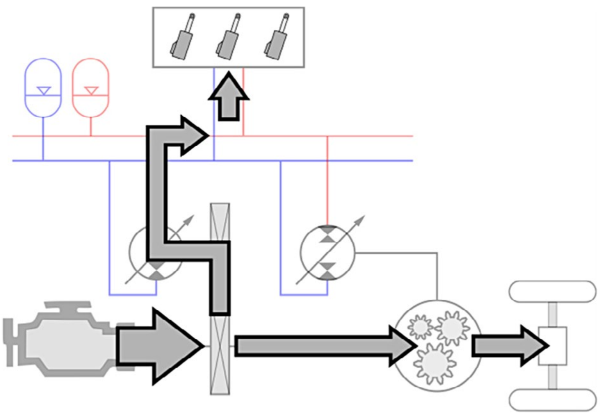

Figure 5. Full mechanical point when work functions and driveline output positive power and SOC is kept constant.

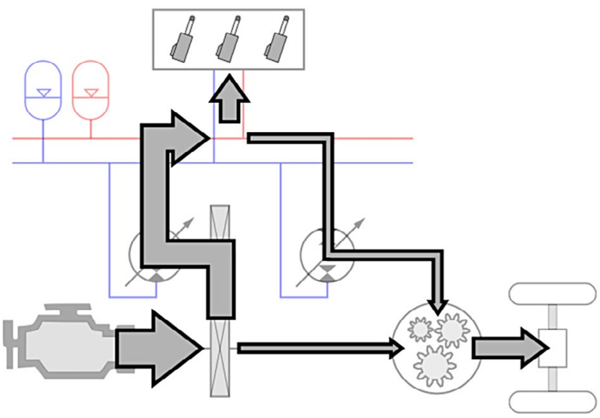

Figure 6. Additive power flow when work functions and driveline output positive power and SOC is kept constant.

of today's wheel loader transmissions. The power flows in the transmission concept are shown schematically in Figure 3.

At low speeds in the power-split mode (*F*1 and *R*1), *PM*2 operates as a pump transmitting the power back to the CPR. This operating phase is often called 'negative circulating' power (Renius and Resch 2005). During this phase, the efficiency of the power-split transmission is generally low since energy is continuously lost in the recirculation. In the proposed hybrid concept, however, recirculating power is transferred to the CPR and may be consumed by the work functions or the energy storage. In effect, some or all of the recirculating power is never fed back to *PM*1. Figure 4 shows two cases of negative circulating power when the power consumption of the work functions is positive.

In both cases, *PM*1 transmits less power than is consumed by the work functions since *PM*2 supplies some or all of the power. This has a positive effect on the system efficiency when compared to a system with separated subsystems. Furthermore, the sizing requirements on *PM*1 are also greatly reduced since the work hydraulics are partially supplied by *PM*2. Coming back to Figure 3, when increasing the speed of the machine the angular speed of *PM*2 and the amount of hydraulic power are reduced until the transmission reaches the 'full mechanical point' where *PM*2 is at standstill, see Figure 5.

When the machine speed increases further the transmission enters the 'additive' phase where *PM*2 operates as a motor transmitting power from the CPR to the planetary gear as shown in Figure 6.

At this phase *PM*1 supplies both work functions and driveline with hydraulic power, which makes the power demand high. However, since this phase occurs at a higher speed range, full output power is not required for the work functions. At higher machine speeds, the transportation modes, *F*2 and *F*3, are activated. The power is then transmitted fully mechanically in the same manner as at the full mechanical point in the power-split modes (Figure 5). During the transportation modes *PM*2 is completely disconnected. The driveline architecture then fully corresponds to a parallel hybrid architecture for both driveline and work functions, see Filla (2009).

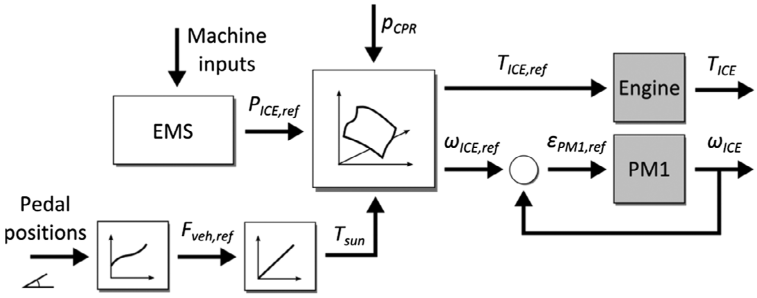

Figure 7. Example of control approach of the supply system.

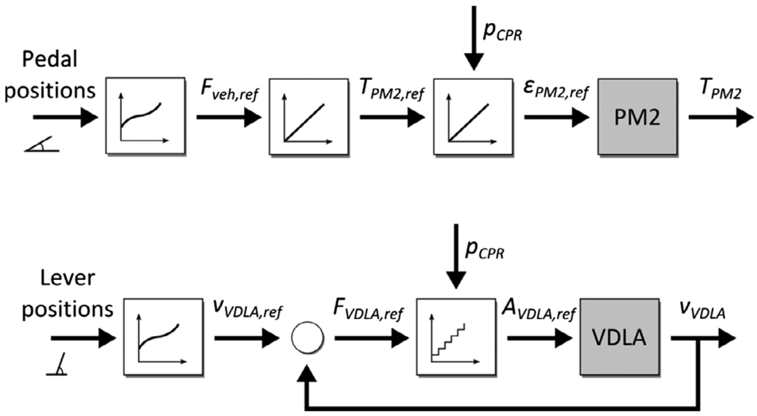

Figure 8. Control approach of PM2 and the VDLAs (steering, boom and bucket).

Control aspects

In this section control aspects of the proposed concept are briefly discussed and one control approach is suggested. Figure 7 shows a possible control implementation for the supply system.

A high-level Energy Management Strategy (EMS) determines the split between engine power and accumulator power. If the requested engine power is higher than the demanded machine output power the State-of-Charge (SOC) will increase and vice versa. Based on the reference engine power, $P_{\text{ICE, ref}}$, the system pressure, p_{CPR}, and the sun gear torque, T_{sun}, the optimal engine speed and torque can be determined. This is a non cycle-dependent optimisation which considers the engine efficiency map as well as the efficiency of *PM*1. In this example the engine is torque-controlled in an open loop and *PM*1 is speed-controlled in a closed loop to achieve the determined operating point. However, it is also possible to switch tasks depending on the capabilities of the respective control unit.

Figure 8 shows possible control principles for PM2 and the VDLAs. In the power-split mode *PM*2 is torque controlled from a reference tractive force, $F_{\text{veh, ref}}$, demanded by the operator. This corresponds to the tractive force control conventionally preferred and used in wheel loader powertrains. The work functions are controlled to track a speed reference, $v_{\text{VDLA, ref}}$, given by the operator input. The speed, v_{VDLA}, is controlled in a closed loop by matching a suitable cylinder area

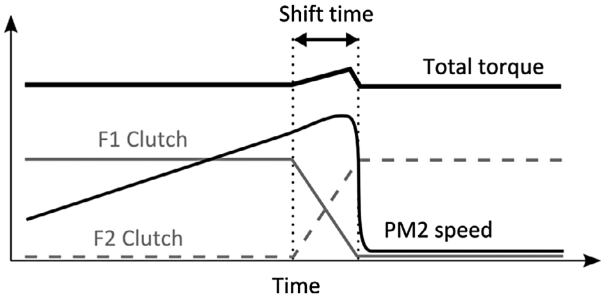

Figure 9. Shift sequence from *F*1 to *F*2.

setting, $A_{\text{VDLA, ref}}$, to the reference force, $F_{\text{VDLA, ref}}$. This is a brief description on the control principle whereas more detailed analysis on the control of multi-chambers cylinders can be found in for instance (Linjama *et al.* 2009).

The described approach above is much similar to the three-level hierarchical control proposed in Li and Mensing (2010) and Cheong *et al.* (2014). Here, the EMS represents the high level, the control of the supply system represents the middle level and the actuator control represents the low level. Similar ideas are also found for electric complex hybrids (Kimura *et al.* 1999), Liu and Peng (2006).

For the transportation modes, *F*2 and *F*3, the engine speed is simply determined by the machine speed while *PM*1 controls the accumulator power with the input from the EMS. The mode shifting sequence between *F*1 and *F*2, however, is a more challenging control problem.

A control principle is shown in Figure 9 where the transferred torque from *PM*2 is reduced by disengaging the *F*1 clutch while engaging the *F*2 clutch.

With a reducing torque, the displacement of *PM*2 is also reduced. When *F*1 is completely released *PM*2 is speed controlled to standstill. The timing is crucial since *PM*2 risks overspeeding if *F*1 is disengaged too early and *PM*2 still operates with a high displacement. When shifting down, *PM*2 must accelerate and synchronise the speed before engaging the clutch. This type of reconnection of a hydraulic motor is studied and tested in Sannelius *et al.* (1999) for a two-motor hydrostatic transmission.

Simulation

This section describes the simulation of the proposed hybrid concept and discusses the control strategy for the complete system. The simulation is based on a quasi-static system model and backwards-facing calculations from a prescribed operating cycle from real-world measurements. The main reason for using backwards-facing simulation is to avoid the reference tracking control problem and put focus on the high level control of the SOC of the hydraulic accumulator. The potential of the system architecture can then be examined in a simple way without developing complex control algorithms.

Modelling

This section describes the component models from a backwards-facing perspective. The models are kept simple, but with consideration to the main power losses to be able to assess the complete system's energy efficiency. The parameters are specified in SI units if not stated otherwise.

Work functions

The VDLAs are each modelled with an idealised variable cylinder area and a prescribed constant efficiency, η_{VDLA}, derived from simulations in previous studies (Heybroek and Norlin 2015). This is a simplification that ignores all the aspects of valve switching and pressure regulation associated with digitally controlled multi-chamber cylinders. This is justified since the dynamics of these aspects are of a much higher order than those of interest on a complete machine level. The speed, v, and force, F, of the linear actuators are given in the pre-recorded operating cycle and the cylinder area, A, is therefore a direct consequence of the current CPR pressure, p_{CPR}, and low side pressure, p_{LP}, according to Equation (1):

$$A_{\{\text{steer, boom, bucket}\}} = \frac{F_{\{\text{steer, boom, bucket}\}}}{(p_{\mathrm{CPR}} - p_{LP})\eta^{i}_{\mathrm{VDLA}}} \tag{1}$$

where i = 1 for positive output power and i = *−1* for returning power. The flow, Q, for each function is calculated according to Equation (2):

$$Q_{\{\text{steer, boom, bucket}\}} = v_{\{\text{steer, boom, bucket}\}} A_{\{\text{steer, boom, bucket}\}} \tag{2}$$

Axles and wheels

The axles and wheels are modelled with a fixed gear ratio, i_0, a static rolling radius, r_{tire}, and a constant efficiency, η_{axle}, according to Equations (3) and (4):

$$\omega_{\mathrm{prop}} = \frac{v_{\mathrm{wheel}}}{r_{\mathrm{tire}} i_0} \tag{3}$$

$$T_{\mathrm{prop}} = \frac{F_{\mathrm{wheel}} r_{\mathrm{tire}} i_0}{\eta^{i}_{\mathrm{axle}}} \tag{4}$$

where ω_{prop} is the propeller shaft speed, T_{prop} is the propeller shaft torque and $i = \pm 1$ according to the above.

Driveline mechanics

The required torque acting on the sun gear is calculated with Equation (5) for the power-split modes:

$$T_{\mathrm{sun}} = i_{\{F1,R1\}} \frac{T_{\mathrm{prop}}}{\eta^{i}_{\mathrm{tra}}(1-R)} \tag{5}$$

where $i_{\{F1,R1\}}$ is the gear ratio of the spur gears for *F*1 and *R*1 modes, R is the planetary gear ratio, η_{tra} is the transmission efficiency and $i = \pm 1$ according to the above. The required speed and torque of *PM*2 is calculated with Equations (6) and (7) for the power-split modes:

$$T_{PM2} = i_{\{F1,R1\}} i_{PM2} \frac{T_{\mathrm{prop}}}{\eta^{i}_{\mathrm{tra}}(1/R-1)} \tag{6}$$

$$\omega_{PM2} = \frac{1}{i_{PM2}} \left(\frac{\omega_{\mathrm{prop}}(1-1/R)}{i_{\{F1,R1\}}} + \frac{\omega_{\mathrm{ICE}}}{R} \right) \tag{7}$$

where ω_{ICE} is the engine speed and i_{PM2} is the gear ratio for *PM*2. The speed of *PM*1 is given by Equation (8):

$$\omega_{PM1} = \omega_{\mathrm{ICE}} i_{PM1} \tag{8}$$

Pumps/motors

The pumps/motors, *PM*1 and *PM*2, are modelled with standard torque and flow relations according to Equations (9) and (10):

$$T_{PM\{1,2\}} = \frac{\varepsilon_{PM\{1,2\}} D_{PM\{1,2\}} (p_{\mathrm{CPR}} - p_{LP})}{2\pi \eta^{i}_{hm,PM\{1,2\}}} \tag{9}$$

$$Q_{PM\{1,2\}} = \varepsilon_{PM\{1,2\}} D_{PM\{1,2\}} n_{PM\{1,2\}} \eta^{i}_{\mathrm{vol},PM\{1,2\}} \tag{10}$$

where ε is the relative displacement, D is maximum displacement and $i = \pm 1$ for pump or motor operation. The volumetric efficiency, η_{vol}, and the hydromechanical efficiency, η_{hm}, are modelled with polynomial expressions with respect to pressure, speed and relative displacement according to the method described in Mikeska (2002).

Engine

The engine fuel consumption, m_{fuel}, is modelled with a look-up map depending on engine torque and speed according to Equation (11):

$$\dot{m}_{\mathrm{fuel}} = f(\omega_{\mathrm{ICE}}, T_{\mathrm{ICE}}) \tag{11}$$

The engine speed is given by Equation (12):

$$\omega_{\mathrm{ICE}} = \int \frac{1}{J_{\mathrm{ICE}}} \left(T_{\mathrm{ICE}} - T_{PM1} i_{PM1} - T_{\mathrm{sun}}\right) \mathrm{d}t \tag{12}$$

A maximum torque curve limits the requested engine torque, T_{ICE}. The efficiency map of the engine and the maximum torque curve are shown in the results section.

Energy storage

The high-pressure accumulator is modelled assuming a completely adiabatic process for charging and discharging. A cycle efficiency factor is used in the model to represent the losses of the accumulator. The accumulator capacitance is assumed to represent the complete compressibility of the CPR. The accumulator pressure is thus equal to the CPR pressure given by Equation (13):

$$p_{\mathrm{CPR}} = \frac{p_0 V_0^{\gamma}}{V^{\gamma}} \tag{13}$$

where p_0 is the accumulator precharge pressure, V_0 is the total accumulator volume and γ is the polytropic index. The gas volume, V, is given by Equation (14):

$$V = V_0 - \int Q_{\mathrm{acc}} \eta_{\mathrm{acc}}^{i} \mathrm{d}t \tag{14}$$

where Q_{acc} is the flow to the accumulator, η_{acc} is the constant accumulator efficiency and $i = \pm 1$ for charging/discharging of the accumulator. The flow to the accumulator is calculated according to Equation (15):

$$Q_{\mathrm{acc}} = Q_{PM1} - Q_{PM2} - Q_{\mathrm{steer}} - Q_{\mathrm{boom}} - Q_{\mathrm{bucket}} \tag{15}$$

The low pressure accumulator is assumed to be a constant pressure source to avoid additional system states. This simplified model is justified since the energy content is relatively low compared to the high-pressure accumulator.

Energy management strategy

Energy management strategies have been extensively studied for on-road electric hybrid vehicles as well as hydraulic hybrids for various on-road vehicles. Less work, however, has been done for off-road vehicles and construction machines, in particular where multiple subsystems are hybridised. Typical wheel loader operation is highly transient with quick accelerations and decelerations and frequent starts and stops. Recuperating and releasing stored energy, from both work functions and driveline, will consequently result in high power flows to and from the energy storage. Another key aspect is that the SOC of a hydraulic accumulator is coupled to its working pressure, in contrast to an electric energy storage where the voltage level is relatively constant. This means that the transferable power of the system is reduced when the accumulator is not fully charged. The EMS must therefore also take into account the required power output of the actuators and cannot be controlled solely to optimise fuel efficiency. In (Kumar and Ivantysynova 2011) this issue is addressed and a strategy is proposed based on a minimum pressure profile as a function of vehicle speed to achieve sufficient performance and a high degree of braking energy recuperation. In (Wang *et al.* 2016) some of the aspects of the design of an EMS for off-road vehicles is also demonstrated.

A common methodology used in literature is to formulate a deterministic Dynamic Programming (DP) algorithm to obtain the optimal EMS for a specific drive cycle. The sequential nature of the optimisation algorithm is powerful for making optimal control decisions in a discrete time series. Although it requires complete knowledge of the drive cycle in advance, the resulting strategy is not suitable for real-time implementation. The results from such optimisation are instead commonly used as a comparison to a non-cycle-dependent optimal control strategy, as in Liu and Peng (2006) and Ayalew and Molla (2011) or simply to gain knowledge about how to construct a rule-based EMS, as in Wu *et al.* (2004), and Cheong *et al.* (2014). See Karbaschian and Söffker (2014) for more details and a comprehensive overview of methodologies for optimal control strategies for (hydraulic) hybrid vehicles. In this paper, DP is used to understand the potential of the proposed system architecture and to gain knowledge about the optimal EMS and the power flows of the system.

Optimisation problem

From Equations (12) and (14) two time-dependent system states are defined according to Equations (16) and (17):

$$x_1(t) = \frac{\omega_{ICE}(t) - \omega_{ICE,\,min}}{\omega_{ICE,\,max} - \omega_{ICE,\,min}} \tag{16}$$

$$x_2(t) = \frac{p_{\mathrm{CPR}}(t) - p_0}{p_{\max} - p_0} \tag{17}$$

where p_{max} is the maximum accumulator pressure and $\omega_{ICE,\,min}$ and $\omega_{ICE,\,max}$ are the minimum and maximum engine speeds. The control signals are defined according to Equations (18) and (19):

$$u_1(t) = \frac{T_{\mathrm{ICE}}(t)}{T_{\mathrm{ICE,\,max}}} \tag{18}$$

$$u_2(t) = \varepsilon_{PM1}(t) \tag{19}$$

A positive relative displacement, ε_{PM1}, corresponds to pumping mode where flow is supplied to the CPR and a negative value corresponds to motoring mode where flow is taken from the CPR. The optimisation problem is mathematically formulated according to Equation (20):

$$min \int_0^{t_f} \dot{m}_{\mathrm{fuel}}(\boldsymbol{u}(t))\mathrm{d}t \tag{20}$$

subject to

$$\dot{\boldsymbol{x}} = F(\boldsymbol{x}(t),\, \boldsymbol{u}(t),\, t) \tag{21}$$

$$0 \le x_1(t) \le 1 \tag{22}$$

$$0 \le x_2(t) \le 1 \tag{23}$$

$$0 \le u_1(t) \le 1 \tag{24}$$

$$-1 \le u_2(t) \le 1 \tag{25}$$

$$x_1(0) = 0.5 \tag{26}$$

$$x_2(0) = 0.5 \tag{27}$$

$$x_2(t_f) > 0.5 \tag{28}$$

where $\boldsymbol{x}$ is the system state vector, $\boldsymbol{u}$ is the control signal vector and t_f is the final time. The objective function is discretised according to Equation (29):

$$\int_0^{t_f} \dot{m}_{\mathrm{fuel}}(\boldsymbol{u}(t))\mathrm{d}t = \sum_{k=0}^{N-1} m_{\mathrm{Fuel}}\left(\boldsymbol{x}_k,\, \boldsymbol{u}_k,\, t_k\right) \tag{29}$$

where k is the time index and N is the number of time steps in the operating cycle. The system states are updated each time step according to Eq. (30):

$$\boldsymbol{x}_{k+1} = f(\boldsymbol{x}_k,\, \boldsymbol{u}_k,\, t_k) \tag{30}$$

where the function $f(\boldsymbol{x}_k, \boldsymbol{u}_k, t_k)$ updates the states for each time step according to Figure 10.

The flows from the VDLAs are given directly from the operating cycle, according to Equations (1) and (2). For a given engine speed and pressure the flow of $PM2$ is calculated with Equations (6), (7), (9) and (10). The

Table 1. Main simulation parameters.

Maximum engine power	P_{ice}	90 kW
Maximum engine speed	$\omega_{\mathrm{ice,\,max}}$	2200 rpm
Minimum engine speed	$\omega_{\mathrm{ice,\,min}}$	600 rpm
Engine inertia	J_{ICE}	2.0 kgm^2
$PM1$ maximum displacement	D_{PM1}	192 cm^3/rev
$PM2$ maximum displacement	D_{PM2}	205 cm^3/rev
HP accumulator size	V_0	10 L
Maximum pressure	p_{max}	450 bar
Low side pressure	p_{LP}	30 bar
Tyre radius	r_{tire}	0.70 m
Planetary gear ratio	R	−1.9
Gear ratio $PM1$	i_{PM1}	1.0
Gear ratio $PM2$	i_{PM2}	−0.68
$F1$ speed gear ratio	i_{F1}	0.62
$R1$ speed gear ratio	i_{R1}	−0.74
Axle ratio	i_0	0.047
Axle efficiency	η_0	0.92
Transmission efficiency	η_{tra}	0.96
VDLA efficiency	η_{VDLA}	0.85
Accumulator efficiency	η_{acc}	0.95

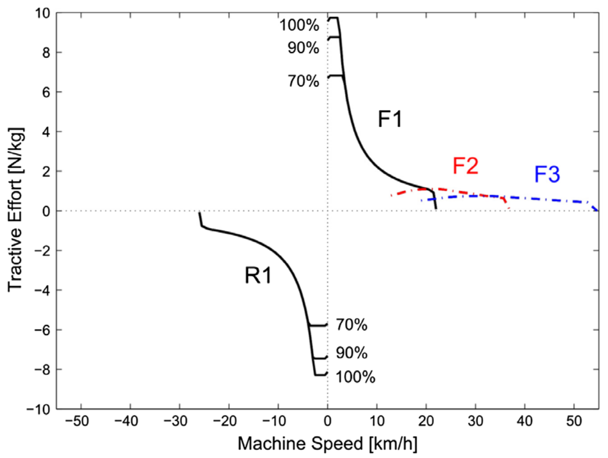

Figure 11. Performance diagram of the proposed hybrid concept at 70, 90 and 100% of the maximum system pressure.

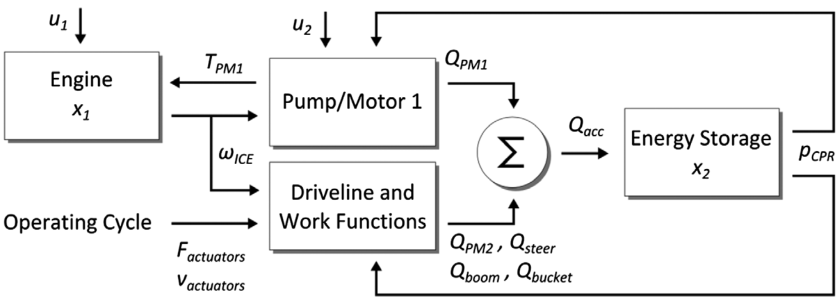

Figure 10. Description of the complete system model and signals.

flow of $PM1$ is calculated using Equations (8) and (10). Finally the system pressure and SOC are updated using Equations (13)–(15). Since the simulation is based on backwards-facing simulation, the actuators are forced to perform the prescribed operating cycle for a certain set of states. The control level of the reference tracking problem, as described in for instance (Cheong *et al.* 2014) and (Li and Mensing 2010), is thereby removed.

Simulation parameters

The main simulation parameters for the hybrid concept are shown in Table 1. Note that all parameters are not shown in SI units to increase the quantity recognition.

The design is done to match the performance of a typical baseline machine of the same size. The hybrid concept is designed with a downsized engine corresponding to around 70% of a baseline machine. The tractive force of the vehicle is dependent on the CPR pressure and consequently the SOC. The maximum displacements of the pumps/motors are therefore sized to meet the tractive effort when operating at a pressure lower than the maximum system pressure. Figure 11 shows the force/speed diagram of the hybrid concept with respect to its machine weight.

The reverse gear ratio, i_{R1}, is sized to achieve 25 km/h in reverse speed, which is assumed to be enough for the reference machine. This results in a slightly lower reverse tractive force at stall relative to the forward range. This is acceptable since traction is nonetheless limited by the friction coefficient between the wheels and the ground. The transportation modes, $F2$ and $F3$, are used to fulfil the maximum required speed of the machine.

The simulated operating cycle is the well-known 'short loading cycle' typical of a production wheel loader. Briefly explained, the wheel loader repetitively approaches and fills the bucket from a gravel pile, reverses and unloads the gravel into a load receiver. See Filla (2009) for a description of the different phases and an illustration of the short loading cycle.

Results

The simulation model described above is implemented in a Matlab m-file and the EMS is optimised using the Matlab script published in Sundström and Guzzella (2009). The time step of the operating cycle is 0.2 s and the length of the cycle is 26 s. Figure 12 shows the main powers of the motion system and the relative displacements of $PM1$ and $PM2$.

The cycle is here divided into six phases describing the main tasks of the wheel loader. In phases 1, 3 and 4 the driveline mainly operates in additive power flow (see Figure 6), where $PM2$ supplies part of the tractive power, which has a positive impact on the transmission efficiency. In phase 2, the bucket filling operation, the driveline operates with negative circulating power (see Figure 4), where $PM2$ transfers power from the driveline

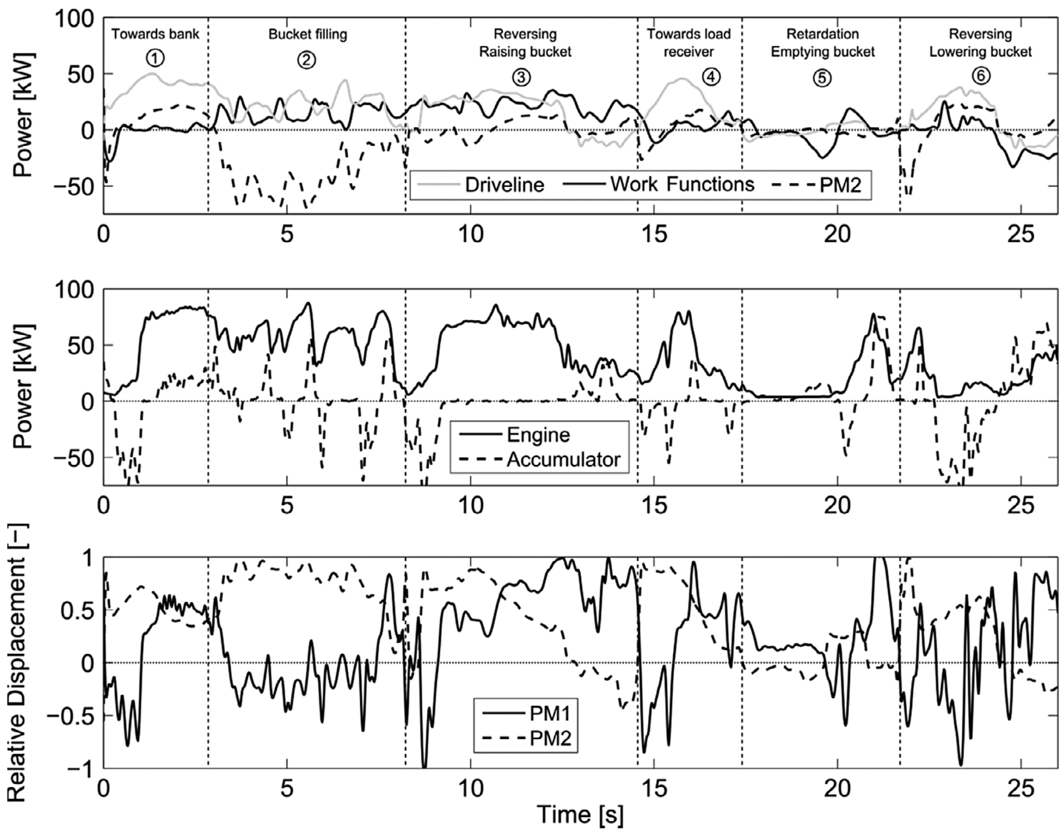

Figure 12. Simulation results of the DP algorithm for the short loading cycle.

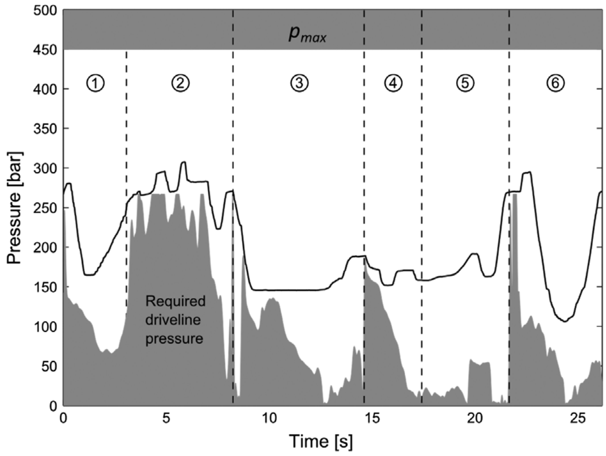

Figure 13. The optimal control of the CPR pressure for the short loading cycle. The dark shaded areas show the infeasible regions.

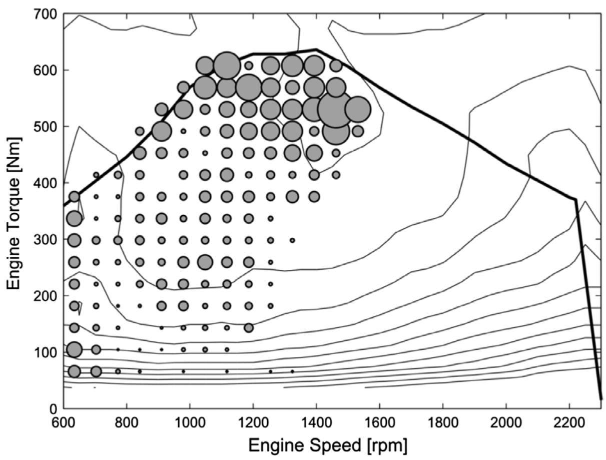

Figure 14. Bubble plot of the engine operating points for the short loading cycle.

back to the CPR. As shown in the figure, some of the recirculating power is used to supply the work functions (Figure 4(a)) and *PM*1 consequently operates with negative displacements. In phase 3, braking power is used directly to power the boom function without loading the energy storage. In phase 6, the machine is decelerated and the boom is lowered at the same time. In this phase, both subsystems supply a high amount of returning energy that is not currently wanted by other functions and therefore needs to be stored in the accumulator. Figure 13 shows the accumulator pressure corresponding to the SOC of the energy storage for the reference cycle.

The required driveline pressure is also shown where *PM*2 is unable to produce the specified tractive force of the operating cycle, according to Equation (9). The required pressure for the work functions was in this simulation not a limiting factor for the EMS.

Figure 14 shows a bubble plot of the operating points of the engine. The operating points of the engine are in general in the high-efficiency region or at low power output to minimise the power losses. The hybrid functionality decoupling engine and load allows the engine to avoid high speeds with low efficiency completely.

Discussion

The driveline configuration of the hybrid concept has the advantages of power-split technology in terms of high efficiency and wide range torque/speed ratio compared to pure series hybrid architectures. Additionally, the circulating power is here shown to be an advantage for the complete motion system, since the work functions are powered directly from *PM*2. This increases the efficiency of the driveline and may allow for a downsizing of the total installed hydraulic displacement when comparing to a concept with separated subsystems. This situation is expected to occur frequently for a wheel loader, since the work functions are commonly used during low-speed operation. Additional power-split modes could increase the transmission efficiency further. However, the rather simple gear configuration of the proposed concept is sufficient for a medium-size wheel loader.

The direct connection through the CPR of all machine actuators enables easy energy recuperation between the functions. A typical short loading cycle includes several phases where energy is returned from one function while another outputs power. The EMS optimisation gives an ideally controlled system pressure level with respect to the simulated operating cycle. In general, the pressure is controlled to be kept as low as possible to increase the efficiency of the components, i.e. to work with as high displacements as possible. The transient behaviour of the wheel loader, however, causes sudden increases in the required pressure level that have to be handled by the EMS. Due to the high capacitance of the hydraulic circuit, the pressure has to be built up well in advance of the peaks. In reality, this would be difficult to accomplish without a predictive control algorithm to avoid compromising the machine performance. One possible way of implementation is to size the components to allow for a pressure window in which the motion system meets the maximum performance requirements. That pressure range can then be used by the EMS in a free manner to optimise the fuel efficiency. With this freedom the EMS could be based on the potential and kinetic energy stored in the machine body, e.g. keep a low SOC when travelling at high speed or having the bucket in a high position to make room for the energy recuperation.

As understood, the design of a hydraulic hybrid system with directly connected energy storage is challenging since the EMS directly affects the transferable power of the motion system. For an optimal concept design the energy management must be treated in parallel to the sizing of components, in particular for heavy machines with transient behaviour.

Conclusions

The proposed hybrid concept is one step towards an efficient hybrid motion system for mobile working machines with several power consumers. The simulation and control optimisation of the system demonstrate the advantages of using a common secondary controlled hydraulic circuit for the propulsion and work functions of a wheel loader. The use of a power-split gear configuration in the driveline renders additional advantages in terms of high efficiency and handling of circulating power. The input-coupled power-split configuration is shown to be of particular advantage when it comes to circulating power at low speeds. A different driveline concept, such as output-coupled power-split, could be useful to adapt the performance to another machine size or to improve fuel efficiency further. Other types of secondary controlled systems, such as transformer-based systems, can also be considered for the work functions. The simplified models for the VDLAs are the main limitations for a full energetic assessment of the concept. More detailed simulation and the development of an online EMS are, however, subjects for future work.

Disclosure statement

No potential conflict of interest was reported by the authors.

Funding

This work was supported by the Swedish Energy Agency [39367-1] under the Swedish Vehicular Research Program (FFI).

Notes on contributors

Karl Pettersson received his MSc degree in Mechanical Engineering from Linköping University, Sweden in 2009. He continued at the university as a PhD student in the division of Fluid and Mechatronic Systems. In 2013 he received his Licentiate degree within design automation of hydromechanical transmissions. He is now working at Volvo Construction Equipment with the focus on the design and control of hydromechanical hybrid drivelines.

Kim Heybroek received his MSc degree from Linköping University, Sweden, in Mechanical Engineering in 2006. In 2008 he received his Licentiate Degree at the division of Fluid and Mechatronics Systems. In 2008 he was with Volvo Construction Equipment in Eskilstuna as a hydraulics design engineer mainly dealing with valve technologies for wheel loaders. In 2010 he joined the Emerging Technologies department, where he is currently working with electro-hydraulics and new machine concepts.

Per Mattsson received his MSc degree 1988 in Mechanical Engineering at Lund University of Technology and his PhD degree 1996 in Machine and Vehicle Design at Chalmers University of Technology, Göteborg. He has been working for 20 years with transmission development at Volvo Cars, Volvo Trucks and Volvo Construction Equipment. Main research interest is power-split CVTs with several modes.

Petter Krus is a professor in Fluid and Mechatronic Systems at Linkoping University. Research interests are fluid power, mechanical and mechatronic systems technology, specifically focusing on system dynamics, control, system simulation, optimisation, system design and design automation. Applications are in aircraft design, road vehicles and construction machinery

ORCID

Petter Krus http://orcid.org/0000-0002-2315-0680

References

Achten, P.A.J., 2008. A serial hydraulic hybrid drive train for off-road vehicles. *Proceedings of the national conference on fluid power*, 51, 515–521.

Ayalew, B. and Molla, S.K., 2011. Power management strategies for a series hydraulic hybrid drivetrain. *International journal of powertrains*, 1 (1), 93–116.

Cheong, K.L., *et al.*, 2014. Hierarchical control strategy for a hybrid hydro-mechanical transmission (HMT) powertrain. *American control conference (ACC)*. Portland, OR, 4599–4604.

Filla, R., 2009. Hybrid power systems for construction machinery: aspects of system design and operability of wheel loaders. *ASME 2009 international mechanical engineering congress and exposition. Lake Buena Vista, FL*, Vol. 13, 611–620.

Heybroek, K. and Norlin, E., 2015. *Hydraulic multi-chamber cylinders in construction machinery*. Linköping: Hydraulikdagarna 2015.

Heybroek, K., Vael, G. and Palmberg, J.-O., 2012. Towards resistance-free hydraulics in construction machinery. *8th international fluid power conference*, Dresden, Germany.

Inderelst, M., *et al.*, 2011. Energy efficient system layout for work hydraulics of excavators. *12th Scandinavian international conference on fluid power*, Tampere, Finland.

Karbaschian, M.A. and Söffker, D., 2014. Review and comparison of power management approaches for hybrid vehicles with focus on hydraulic drives. *Energies*, 7 (6), 3512–3536.

Kimura, A., Abe, T. and Sasaki, S., 1999. Drive force control of a parallel-series hybrid system. *JSAE review*, 20 (3), 337–341.

Kumar, R. and Ivantysynova, M., 2011. An instantaneous optimization based power management strategy to reduce fuel consumption in hydraulic hybrids. *International journal of fluid power*, 12 (2), 15–25.

Li, P.Y. and Mensing, F., 2010. Optimization and control of a hydro-mechanical transmission based hybrid hydraulic

passenger vehicle. *7th international fluid power conference*, Aachen, Germany.
Linjama, M., *et al.*, 2009. Secondary controlled multi-chamber hydraulic cylinder. *11th Scandinavian international conference on fluid power*, Linköping, Sweden.
Liu, J. and Peng, H., 2006. Control optimization for a power-split hybrid vehicle. *American control conference (AAC)*, Portland, OR, 466–471.
Mikeska, D., 2002. A precise steady-state model of displacement machines for the application in virtual prototyping of power-split drives. *2nd FPNI – PhD symposium*, Modena, Italy.
Pettersson, K. and Tikkanen, S., 2009. Secondary control in construction machinery – design and evaluation of an excavator swing drive. *11th Scandinavian international conference on fluid power*, Linköping, Sweden.
Renius, K.T. and Resch, R., 2005. Continuously variable tractor transmissions. *Agricultural equipment technology conference, ASAE distinguished lecture no. 29*, 14–16 February 2005, Louisville, Kentucky, USA, 1–37. American Society of Agricultural Engineers.
Sannelius, M., Rydberg, K.-E. and Palmberg, J.-O., 1999. Hydrostatic transmissions for wheel loaders – an experimental study of a multiple-motor concept. *4th JHPS international symposium on fluid power*, Tokyo, Japan.
Sipola, A., *et al.*, 2008. *Digital hydraulic system*. s.l. Patent no. US 9021798.
Stein, G. et al., 2013. Fuel efficiency in construction equipment – optimize the machine as a system. *International commercial powertrain conference*, Graz, Austria.
Sundström, O. and Guzzella, L., 2009. A generic dynamic programming Matlab function. *IEEE international conference on control applications & intelligent control*, St. Petersburg, Russia, Issue 7, 1625–1630.
Wang, F., *et al.*, 2016. Energy management strategy for a power-split hydraulic hybrid wheel loader. Proceedings of the institution of mechanical engineers, Part D: journal of automobile engineering, 230 (8), 1105–1120.
Wei, S., *et al.*, 2013. Parameter matching analysis of hydraulic hybrid excavators based on dynamic programming algorithm. *Journal of applied mathematics*, 2013, 10.
Wu, B., *et al.*, 2004. Optimal power management for a hydraulic hybrid delivery truck. *Vehicle system dynamics*, 42 (1–2), 23–40.